

## Towards a determination of the chiral critical surface of QCD

---

Owe Philipsen<sup>\*†</sup>

*Westfälische Wilhelms-Universität Münster, 48149 Münster, Germany*

*E-mail:* ophil@uni-muenster.de

The chiral critical surface is a surface of second order phase transitions bounding the region of first order chiral phase transitions for small quark masses in the  $\{m_{u,d}, m_s, \mu\}$  parameter space. The potential critical endpoint of the QCD  $(T, \mu)$ -phase diagram is widely expected to be part of this surface. Since for  $\mu = 0$  with physical quark masses QCD is known to exhibit an analytic crossover, this expectation requires the region of chiral transitions to expand with  $\mu$  for a chiral critical endpoint to exist. Instead, on coarse  $N_t = 4$  lattices, we find the area of chiral transitions to shrink with  $\mu$ , which excludes a chiral critical point for QCD at moderate chemical potentials  $\mu_B < 500$  MeV. First results on finer  $N_t = 6$  lattices indicate a curvature of the critical surface consistent with zero and unchanged conclusions. We also comment on the interplay of phase diagrams between the  $N_f = 2$  and  $N_f = 2 + 1$  theories and its consequences for physical QCD.

*5th International Workshop on Critical Point and Onset of Deconfinement - CPOD 2009,  
June 08 - 12 2009  
Brookhaven National Laboratory, Long Island, New York, USA*

---

<sup>\*</sup>Speaker.

<sup>†</sup>In collaboration with Ph. de Forcrand

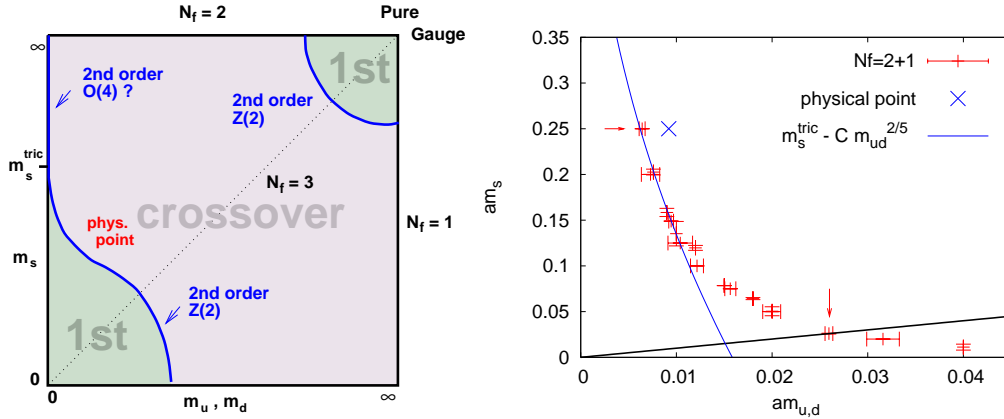


**Figure 1:** Left: Schematic phase transition behaviour of  $N_f = 2 + 1$  QCD for different choices of quark masses ( $m_{u,d}, m_s$ ) at  $\mu = 0$ . Right: Measured chiral critical line on an  $N_f = 4$  lattice with staggered fermions [13].

## 1. Introduction

The QCD phase diagram has been the subject of intense research over the last ten years. Based on asymptotic freedom, one expects at least three different forms of nuclear matter: confined hadronic matter (low  $\mu_B, T$ ), quark gluon plasma (high  $T$ ) and colour-superconducting matter (high  $\mu_B$ , low  $T$ ). Whether and where these regions are separated by true phase transitions has to be determined by first principle calculations and experiments. Since QCD is strongly coupled on scales of nuclear matter, Monte Carlo simulations of lattice QCD are presently the only viable approach.

Unfortunately, the so-called sign problem prohibits straightforward simulations at finite baryon density, thus our expectations for the QCD phase diagram are largely founded on model calculations. Since 2001, several ways have been designed to circumvent the sign problem in an approximate way, all of them valid for  $\mu/T \lesssim 1$  only [1, 2]. Within this range, those methods give quantitatively agreeing results for, e.g., the calculation of  $T_c(\mu)$  [3]. Many phenomenologically interesting quantities like screening masses, the thermodynamical pressure, quark number susceptibilities etc. are thus theoretically controlled at moderate quark densities. On the other hand, because of the intricate and costly finite size scaling analyses involved, determining the order of the QCD phase transition, and hence the existence of a chiral critical point, is a much harder task. Here we discuss the problem of determining the order of the finite temperature phase transition by lattice simulations in the extended parameter space  $\{m_{u,d}, m_s, T, \mu\}$ .

## 2. The chiral critical line at $\mu = 0$

The order of the QCD finite temperature phase transition as a function of quark masses is depicted in Fig. 1, for  $\mu = 0$  (left). In the limits of zero and infinite quark masses (lower left and upper right corners), order parameters corresponding to the breaking of the global chiral and centre symmetries, respectively, can be defined, and one numerically finds first order phase transitions

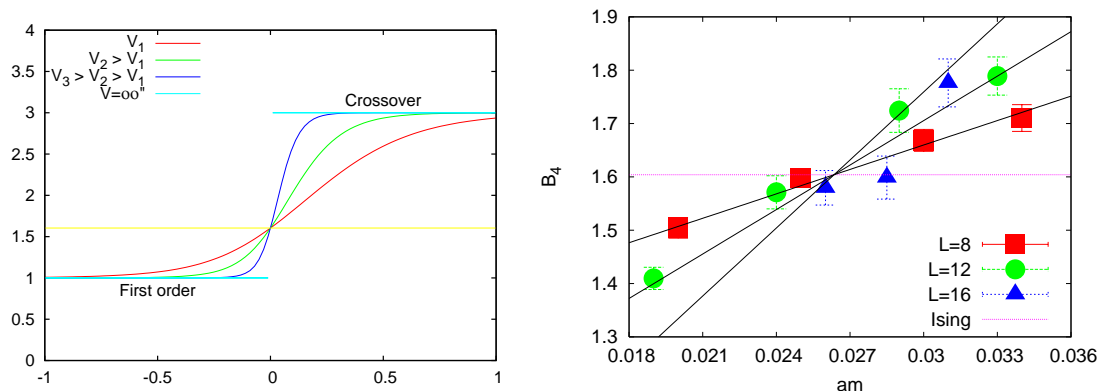


**Figure 2:** Left: Schematic behaviour of the Binder cumulant as a function of the  $N_f = 3$  quark mass at finite and infinite volume. Right: Data obtained on  $N_f = 4$  lattices with staggered fermions [13].

at small and large quark masses at some finite temperatures  $T_c(m_{u,d}, m_s)$ . On the other hand, one observes an analytic crossover at intermediate quark masses, with second order boundary lines separating these regions. Both lines have been shown to belong to the  $Z(2)$  universality class of the 3d Ising model [4, 5, 6]. Since the line on the lower left marks the boundary of the quark mass region featuring a chiral phase transition, it is referred to as chiral critical line.

However, the nature of the  $N_f = 2$  chiral transition is far from being settled. Wilson fermions appear to see  $O(4)$  scaling [7], while staggered actions are inconsistent with  $O(4)$  and  $O(2)$  (for the discretised theory) [8]. A recent finite size scaling analysis using staggered fermions with unprecedented lattice sizes was performed in [9]. Again, these data appear inconsistent with  $O(4)/O(2)$ , and the authors conclude a first order transition to be a possibility. A different conclusion was reached in [10], in which  $\chi$ QCD was investigated numerically. This is a staggered action modified by an irrelevant term such as to allow simulations in the chiral limit. The authors find their data compatible with those of an  $O(2)$  spin model on moderate to small volumes, which would indicate large finite volume effects in the other simulations. Finally, from universality of chiral models it is known that the order of the chiral transition is related to the strength of the  $U_A(1)$  anomaly [11]. In a model constructed to have the right symmetry with a tunable anomaly strength, it has recently been demonstrated non-perturbatively that both scenarios are possible, with a strong anomaly required for the chiral phase transition to be second order [12]. Should the chiral transition turn out to be first order, the likely modification of Fig. 1 (left) would be the disappearance of the tricritical point, with the chiral critical line intersecting the  $N_f = 2$  axis at some finite  $m_{u,d}$  and being  $Z(2)$  all the way.

A convenient observable to locate and identify the second order boundary lines is the Binder cumulant

$$B_4(X) \equiv \langle (X - \langle X \rangle)^4 \rangle / \langle (X - \langle X \rangle)^2 \rangle^2, \quad X = \bar{\psi}\psi. \quad (2.1)$$

It has to be evaluated at the (pseudo-)critical coupling  $\beta_c(m, \mu)$ , i.e. on the phase boundary defined by a vanishing third moment of the fluctuation,  $\langle (X - \langle X \rangle)^3 \rangle|_{\beta_c} = 0$ . In the infinite volume limit,  $B_4 \rightarrow 1, 3$  for a first order transition or crossover, respectively. At the second order transition,  $B_4 \rightarrow 1.604$  dictated by the 3d Ising universality class to which the chiral critical line belongs. On finite

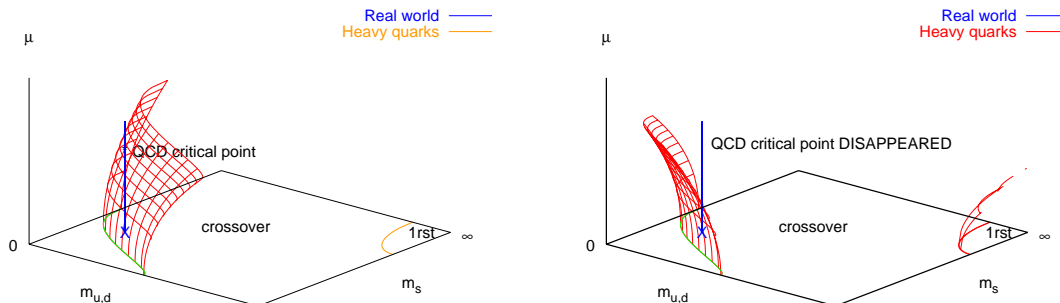


**Figure 3:** Critical surface swept by the chiral critical line as  $\mu$  is turned on. Depending on the curvature, a QCD chiral critical point is present or absent. For heavy quarks the curvature has been determined [6] and the first order region shrinks with  $\mu$ .

lattices this step function gets smeared out to an analytic function, as shown in Fig. 2 (left). The intersection points of different volumes serve as estimators of the critical value,  $B_4(\beta_c(m_c), m_c)$ . A scan of  $B_4(\beta_c(m), m)$  in the  $N_f = 3$  theory is shown in Fig. 2 (right). Also shown is a simultaneous fit of all three volumes to a Taylor expansion of the cumulant around the critical point and exploiting the theoretically known behaviour under finite size scaling,

$$B_4(m, L) = 1.604 + bL^{1/\nu}(m - m_c) + \dots \quad (2.2)$$

Such a fit allows to check whether the chosen volumes are large enough to be consistent with finite size scaling, as well as extracting the universality class from the values of  $B_4$  at the intersection point and the scaling exponent,  $\nu = 0.63$  in the case of 3d Ising.

Following this recipe by fixing  $m_s$  and then scanning in  $m_{u,d}$ , the chiral critical line has recently been mapped out on  $N_t = 4$  lattices [13], Fig. 1 (right). In agreement with expectations, the critical line steepens when approaching the chiral limit. Assuming the  $N_f = 2$  chiral transition to be in the  $O(4)$  universality class implies a tricritical point on the  $m_s$ -axis, Fig. 1 (left). The data are consistent with tricritical scaling [14] of the critical line with  $m_{u,d}$  and we estimate  $m_s^{tric} \sim 2.8T_c$ . However, this value is extremely cut-off sensitive and likely smaller in the continuum, cf. Sec.4.

### 3. The chiral critical surface

When a chemical potential is switched on, the chiral critical line sweeps out a surface, as shown in Fig. 3. According to standard expectations in the literature [14], for small  $m_{u,d}$ , the critical line should continuously shift with  $\mu$  to larger quark masses until it passes through the physical point at  $\mu_E$ , corresponding to the endpoint in the QCD  $(T, \mu)$  phase diagram. This is depicted in Fig. 3 (left), where the critical point is part of the chiral critical surface. However, it is also possible for the chiral critical surface to bend towards smaller quark masses, Fig. 3 (right), in which case there would be no chiral critical point or phase transition at moderate densities. For definiteness, let us consider three degenerate quarks, represented by the diagonal in the quark mass plane. The critical

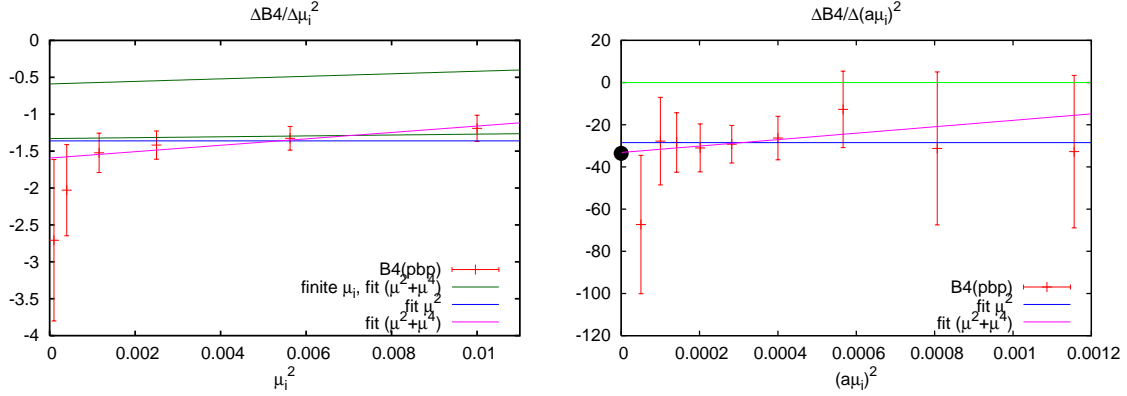


**Figure 4:**  $\mu^2$ -dependence of the Binder cumulant on the chiral critical line for  $N_f = 3$  (left) [15] and  $N_f = 2 + 1$  with physical strange quark mass (right), both for  $N_t = 4$ .

quark mass corresponding to the boundary point has an expansion

$$\frac{m_c(\mu)}{m_c(0)} = 1 + \sum_{k=1} c_k \left( \frac{\mu}{\pi T} \right)^{2k}. \quad (3.1)$$

A strategy to learn about the chiral critical surface is now to tune the quark mass to  $m_c(0)$  and evaluate the leading coefficients of this expansion. In particular, the sign of  $c_1$  will tell us which of the scenarios in Fig. 1 is realised.

The curvature of the critical surface in lattice units is directly related to the behaviour of the Binder cumulant via the chain rule,

$$\frac{dam_c}{d(a\mu)^2} = - \frac{\partial B_4}{\partial (a\mu)^2} \left( \frac{\partial B_4}{\partial am} \right)^{-1}. \quad (3.2)$$

While the second factor is sizeable and easy to evaluate, the  $\mu$ -dependence of the cumulant is excessively weak and requires enormous statistics to extract. In order to guard against systematic errors, this derivative has been evaluated in two independent ways. One is to fit the corresponding Taylor series of  $B_4$  in powers of  $\mu/T$  to data generated at imaginary chemical potential [13, 15], the other to compute the derivative directly and without fitting via the finite difference quotient [15],

$$\frac{\partial B_4}{\partial (a\mu)^2} = \lim_{(a\mu)^2 \rightarrow 0} \frac{B_4(a\mu) - B_4(0)}{(a\mu)^2}. \quad (3.3)$$

Because the required shift in the couplings is very small, it is adequate and safe to use the original Monte Carlo ensemble for  $am^c(0), \mu = 0$  and reweight the results by the standard Ferrenberg-Swendsen method. Moreover, by reweighting to imaginary  $\mu$  the reweighting factors remain real positive and close to 1.

The results of these two procedures based on 20 and 5 million trajectories on  $8^3 \times 4$ , respectively, are shown in Fig. 4 (left). The error band represents the first coefficient from fits to imaginary  $\mu$  data, while the data points represent the finite difference quotient extrapolated to zero. Both results are consistent, and the slope permits and extraction of the subleading  $\mu^4$  coefficient, while the combination of all data also constrains the sign of the  $\mu^6$  term. After continuum conversion

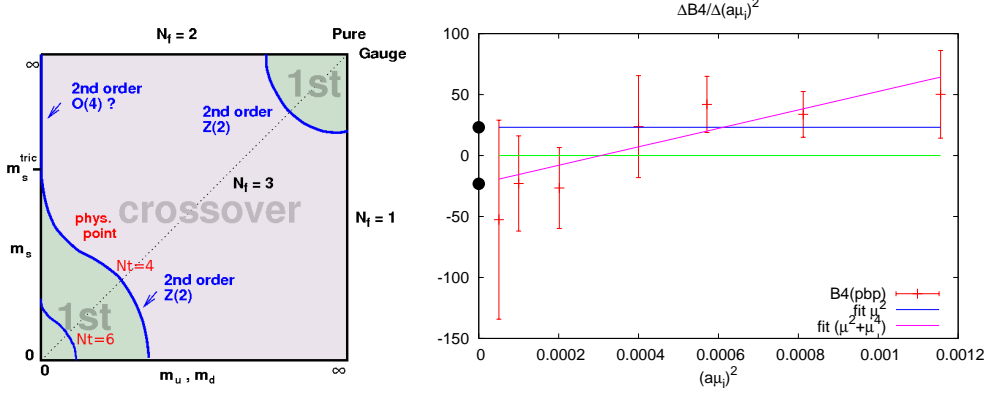


**Figure 5:** Left: The chiral critical line moves to smaller quark masses with decreasing lattice spacing. Right:  $\mu^2$ -dependence of the Binder cumulant on the chiral critical line for  $N_f = 3, N_t = 6$

the result for  $N_f = 3$  is  $c_1 = -3.3(3), c_2 = -47(20), c_3 < 0$  [15]. The same behaviour is found for non-degenerate quark masses. Tuning the strange quark mass to its physical value, we calculated  $m_c^{u,d}(\mu)$  with  $c_1 = -39(8)$  and  $c_2 < 0$ , Fig. 4 (right). Hence, on coarse  $N_t = 4$  lattices, the region of chiral phase transitions shrinks as a real chemical potential is turned on, and there is no chiral critical point for  $\mu_B \lesssim 500$  MeV. Note that one also observes a weakening of the phase transition with  $\mu$  in the heavy quark case [6], in recent model studies of the light quark regime [18, 19], as well as a weakening of the transition with isospin chemical potential [20].

#### 4. First steps towards the continuum, $N_t = 6$

The largest uncertainty in these calculations by far is due to the coarse lattice spacing  $a \sim 0.3$  fm on  $N_t = 4$  lattices. First steps towards the continuum are currently being taken on  $N_t = 6, a \sim 0.2$  fm. At  $\mu = 0$ , the chiral critical line is found to recede strongly with decreasing lattice spacing [16, 17]: for  $N_f = 3$ , on the critical point  $m_\pi(N_t = 4)/m_\pi(N_t = 6) \sim 1.8$ . Thus, in the continuum the gap between the physical point and the chiral critical line is much wider than on coarse lattices, as indicated in Fig. 5 (left). Preliminary results for the curvature of the critical surface, Fig. 5 (right), result in  $c_1 = 7(14), -17(18)$  for a LO,NLO extrapolation in  $\mu^2$ , respectively. Thus the sign of the curvature is not yet constrained. But even if positive, its absolute size appears too small to make up for the shift of the chiral critical line towards smaller quark masses, and one would again conclude for absence of a chiral critical point below  $\mu_B \lesssim 500$  MeV in this approximation. Higher order terms with large coefficients would be needed to change this picture.

Note that on current lattices cut-off effects appear to be larger than finite density effects, hence definite conclusions for continuum physics cannot yet be drawn. A general finding is the steepness of the critical surface, making the location of a possible critical endpoint extremely quark mass sensitive, and hence difficult to determine accurately.

#### 5. The interplay between $N_f = 2, 3$ and $N_f = 2 + 1$

Let us finally comment on the importance of understanding both the  $N_f = 2, 3$  as well as their connection before concluding anything for physical QCD. Fig. 6 (left) shows the scenario that

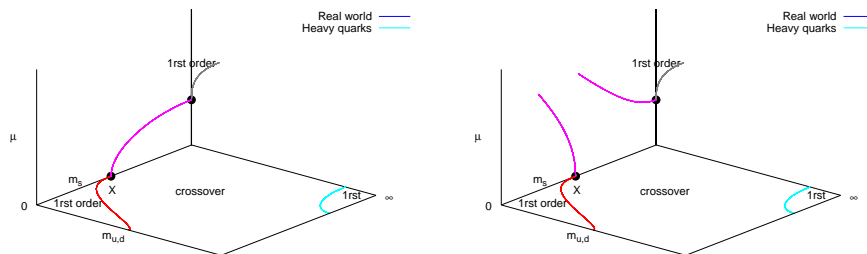


**Figure 6:** Two possible scenarios for connected and disconnected triple lines in the  $m_{u,d} = 0$ -plane.

is used in the literature when the argument for the expected QCD phase diagram with a critical endpoint is made [14]. The tricritical point at  $\mu = 0$ , which we have discussed here, is expected to be analytically connected by a tricritical line, upon varying  $m_s$ , to the tricritical point at some finite  $\mu$  in the two-flavour case. This picture arises plausibly if the chiral critical surface behaves as in Fig. 3 (left). However if, as on our coarse lattices, Fig. 3 (right) is realised, the situation might well be as in Fig. 6 (right). Even if the chiral  $N_f = 2$  theory does feature a tricritical point at finite  $\mu$ , it need not be connected to the chiral critical surface, and nothing follows for the physical point without additional information.

Furthermore, the shrinking of the critical quark masses with diminishing lattice spacing makes it likely that a potential tricritical point, Fig. 1, also moves from a large value for the strange quark mass,  $m_{u,d} = 0, m_s^{tric} \sim 2.8T$  on  $N_t = 4$  [13], towards smaller values in the continuum limit. In particular, it is possible to have a situation for which  $m_{u,d} = 0, m_s^{tric} < m_s^{phys}$ . In this case the chiral critical surface we have been discussing here would not be responsible for a possible critical point, regardless of its curvature, but another surface emanating from the O(4)-chiral limit. Again, both of these scenarios depend on conclusively understanding the situation in the  $N_f = 2$  chiral limit.

## 6. Conclusions

The determination of the order of the QCD finite temperature phase transition as a function of quark chemical potential is a maximally difficult problem. Besides the sign-problem, the strong quark mass and flavour dependence are responsible for potentially rich structures in the  $\{m_{u,d,s}, T, \mu\}$  parameter space which are compute-expensive to disentangle due to the required intricate finite size scaling analyses in the light quark mass regime. The existing results show that we need to control various limiting cases of QCD as well as their connection to  $N_f = 2 + 1$  in order to understand if there is a critical point in the QCD phase diagram, and to which critical surface it belongs.

## Acknowledgements:

This work is partially supported by Deutsche Forschungsgemeinschaft, project PH 158/3-1.

## References

- [1] O. Philipsen, Eur. Phys. J. ST **152** (2007) 29 [arXiv:0708.1293 [hep-lat]]. PoS **LAT2005** (2006) 016 [arXiv:hep-lat/0510077].
- [2] C. Schmidt, PoS **LAT2006** (2006) 021 [arXiv:hep-lat/0610116].
- [3] P. de Forcrand and S. Kratochvila, PoS **LAT2005** (2006) 167 [hep-lat/0509143].
- [4] F. Karsch, E. Laermann and C. Schmidt, Phys. Lett. B **520** (2001) 41 [arXiv:hep-lat/0107020].
- [5] P. de Forcrand and O. Philipsen, Nucl. Phys. B **673** (2003) 170 [arXiv:hep-lat/0307020].
- [6] S. Kim, Ph. de Forcrand, S. Kratochvila and T. Takaishi, PoS **LAT2005**, (2006) 166 [arXiv:hep-lat/0510069].
- [7] A. Ali Khan *et al.* [CP-PACS Collaboration], Phys. Rev. D **63** (2001) 034502 [hep-lat/0008011]; Y. Iwasaki *et al.*, Phys. Rev. Lett. **78** (1997) 179 [hep-lat/9609022].
- [8] C. W. Bernard *et al.* [MILC Collaboration], Phys. Rev. D **61** (2000) 111502 [hep-lat/9912018]; E. Laermann, Nucl. Phys. Proc. Suppl. **60A** (1998) 180.
- [9] M. D'Elia, A. Di Giacomo and C. Pica, Phys. Rev. D **72** (2005) 114510 [hep-lat/0503030].
- [10] J. B. Kogut and D. K. Sinclair, Phys. Rev. D **73** (2006) 074512 [hep-lat/0603021].
- [11] R. D. Pisarski and F. Wilczek, Phys. Rev. D **29**, 338 (1984).
- [12] S. Chandrasekharan and A. C. Mehta, [arXiv:0705.0617 [hep-lat]].
- [13] P. de Forcrand and O. Philipsen, JHEP **0701** (2007) 077 [hep-lat/0607017].
- [14] A. M. Halasz *et al.*, Phys. Rev. D **58** (1998) 096007 [arXiv:hep-ph/9804290].
- [15] P. de Forcrand and O. Philipsen, JHEP **0811** (2008) 012 [arXiv:0808.1096 [hep-lat]].
- [16] P. de Forcrand, S. Kim and O. Philipsen, PoS **LAT2007** (2007) 178 [arXiv:0711.0262 [hep-lat]].
- [17] G. Endrodi *et al.*, PoS **LAT2007** (2007) 182 [arXiv:0710.0998 [hep-lat]].
- [18] K. Fukushima, Phys. Rev. D **78** (2008) 114019 [arXiv:0809.3080 [hep-ph]].
- [19] E. S. Bowman and J. I. Kapusta, Phys. Rev. C **79** (2009) 015202 [arXiv:0810.0042 [nucl-th]].
- [20] J. B. Kogut and D. K. Sinclair, Phys. Rev. D **77** (2008) 114503 [arXiv:0712.2625 [hep-lat]].